ccna-imaging-biomarkers

Release 0.0.1

CCNA team 9

Oct 05, 2021

GENERAL

Warning: This documentation corresponds to the ccna-2020 release. This is a work-in-progress, and not all the imaging biomarkers scheduled for release are included.

350+ clinicians and researchers throughout Canada came together to form the Canadia Consortium on Neurodegeneration in Aging (CCNA) in 2014, with the goal of accelerating progress in research on age-related neurodegenerative diseases, including Alzheimer's disease, Vascular dementia, Frontotemporal dementia, and Lewy body dementia. They have assembled a pan-Canadian cohort on Comprehensive Assessment of Neurodegeneration and Dementia (COMPASS-ND). The current documentation describes an effort of team 9 "discovering new biomarkers" of CCNA, aimed at generating standardized imaging biomarkers for all COMPASS-ND data. These imaging biomarkers are openly shared as part of the CCNA data infrastructure.

CHAPTER

ONE

DATASET

Standardized imaging biomarkers have been generated on the pan-Canadian cohort on Comprehensive Assessment of Neurodegeneration and Dementia (COMPASS-ND), assembled by the CCNA. COMPASS-ND provides an opportunity to study the full spectrum of age-related dementias. Data collection on 2,310 individuals (ages 50-90) is projected to be completed by the end of 2021, and will feature individuals with the following cognitive conditions: AD dementia (N=150), other dementias (N=600), subjective cognitive impairment (N=300), MCI (N=400), vascular-MCI (N=200), and CN (N=660). Currently, 1,132 of 2,310 individuals have been recruited and includes 85 AD dementia and 110 CN individuals. All participants are being deeply phenotyped with extensive clinical, neuropsychological, neuroimaging, biospecimen and neuropathological assessments. Please refer to (Chertkow et al., 2019) for more information on the cohort.

CHAPTER

TWO

ACCESS

The imaging ccna-biomarkers release can be accessed using the SFTP serever of the CCNA LORIS portal. The most update info on CCNA Data Access Policy can be found at https://ccna-ccnv.ca/policies/. For convenience, we have provided a brief outline of the required steps. CCNA investigators may submit request to access/analyze CCNA acquired data to a publication data access committee (PDAC), through CCNA Central. Project/publication summary is provided with the request. Following review of the request CCNA grants access/analysis of CCNA acquired data. For non-CCNA investigators, CCNA data are embargoed for one (1) year after the entire cohort has been completed, uploaded into LORIS, quality controlled and locked. After embargo period, non-CCNA Investigator/CCNA Partner submits request to access CCNA acquired data to PDAC through CCNA Central. Project outline and relevant background material are provided with the request. Moreover, CCNA Partners may ask CCNA investigators to pursue projects on their behalf. PDAC notifies non-CCNA Investigator/CCNA Partner of decision through CCNA Central.

2.1 How to acknowledge

We require that all publications using the CCNA data include the following language in the acknowledgement section:

> The pan-Canadian cohort on Comprehensive Assessment of Neurodegeneration and Dementia (COMPASS-ND) is assembled by the Canadian Consortium on Neurodegeneration in Aging (CCNA) (Chertkow et al., 2019). The Jewish General Research Ethics Board approved the COMPASS-ND study. The CCNA is supported by an infrastructure and operating grant from the CIHR (Grant no. CNA-137794) and the following partners: Alberta Prion Research Institute, Alzheimer's Research UK, Alzheimer Society of Canada, Canadian Nurses Foundation, Fonds de recherche du Québec – Santé, Michael Smith Foundation for Health Research, New Brunswick Health Research Foundation, Nova Scotia Health Research Foundation, Ontario Brain Institute, Pfizer Inc., Robin and Barry Picov Family Foundation, Sanofi, Saskatchewan Health Research Foundation, Women's Brain Health Initiative. The CNNA imaging biomarkers team receives additional support from Alberta Innovates and the Courtois foundation. The CCNA imaging biomarkers have been prepared, validated and documented by investigators within team 9 of CCNA, see the online documentation for an up-to-date list of contributors.

Please include the following reference (Chertkow et al., 2019) along with this description:

> H Chertkow, M Borrie, V Whitehead, S E Black, H H Feldman, S Gauthier, D B Hogan, M Masellis, K McGilton, K Rockwood, M C Tierney, M Andrew, G-Y R Hsiung, R Camicioli, E E Smith, J Fogarty, J Lindsay, S Best, A Evans, S Das, Z Mohaddes, R Pilon, J Poirier, N A Phillips, E MacNamara, R A Dixon, S Duchesne, I MacKenzie, R J Rylett. The Comprehensive Assessment of Neurodegeneration and Dementia: Canadian Cohort Study. Canadian Journal of Neurological Sciences / Journal Canadien des Sciences Neurologiques, Volume 46, Issue 5, September 2019, pp. 499-511.

In addition, we encourage you to include any relevant excerpt from this documentation in your manuscript. Although some journals flag reproductions of technical documentation as plagiarism, using a standardized wording help consistency and reproducibility in the literature. Please reproduce this documentation verbatim to the greatest extent possible, and justify to the editor that this practice does not fall under plagiarism.

2.2 Release version

Multiple versions of the COMPASS-ND imaging biomarkers are released, indicated by year. The current release is *ccna-2020*. Correspondingly, multiple versions of this documentation exist, which can all be accessed in the online version. Please make sure to use excerpts from the correct version of the documentation, matching the data release used in the analysis, and include the name of the CCNA data release used in the analysis (e.g. ccna-2020).

CHAPTER

THREE

AUTHORS

3.1 Overview

Team 9 "discovering new biomarkers" of the Canadian Consortium on Neurodegeneration in Aging (CCNA) is co-lead by Dr Roger Dixon, department of Psychology, University of Alberta, and Dr Pierre Bellec, department of Psychology, University of Montreal. The generation of imaging biomarkers using standardized pipelines is one of the core objective of the CCNA biomarkers team, and involves only a subset of investigators, listed below. These imaging biomarkers cover all imaging modalities collected as part of the "comprehensive assessment of neurodegeneration in aging" (COMPASS-ND) cohort, following the Canadian Dementia Imaging Protocol CDIP.

3.2 Funding

The Canadian consortium on neurodegeneration in aging is supported by an infrastructure and operating grant from the CIHR (Grant no. CNA-137794) and the following partners: Alberta Prion Research Institute, Alzheimer's Research UK, Alzheimer Society of Canada, Canadian Nurses Foundation, Fonds de recherche du Québec – Santé, Michael Smith Foundation for Health Research, New Brunswick Health Research Foundation, Nova Scotia Health Research Foundation, Ontario Brain Institute, Pfizer Inc., Robin and Barry Picov Family Foundation, Sanofi, Saskatchewan Health Research Foundation, Women's Brain Health Initiative. The CNNA imaging biomarkers team receives additional support from Alberta Innovates and the Courtois foundation.

3.3 Standardized Imaging Biomarkers subteam

In alphabetical order:

- Dr. AmanPreet Badhwar, principal investigator (CRIUGM, University of Montreal, Québec, CA).
- Dr. Christian Beaulieu, principal investigator (University of Alberta, Alberta, CA).
- Dr. Pierre Bellec, co-lead (CRIUGM, University of Montreal, Québec, CA).
- Dr. Faisal Beg, principal investigator (Simon Fraiser University, British Columbia, CA).
- Mr. Arnaud Boré, data scientist (CRIUGM and Sherbrooke University, Quebec, CA).
- Dr. Mallar Chakravarti, principal investigator (Douglas Institute, McGill University, Quebec, CA).
- Dr. Louis Collins, principal investigator (Montreal Neurological Institute, McGill University, Quebec, CA).
- Dr. Maxime Descoteaux, principal investigator (Sherbrooke University, Quebec, CA).
- Dr. Roger Dixon, co-lead (University of Alberta, Alberta, CA).

- Dr. Simon Duchesne, principal investigator (Cervo Centre, Laval University, Quebec, CA).
- Dr. Desirée Lussier, post-doctoral fellow (CRIUGM, University of Montreal, Quebec, CA).
- Dr. Eric Smith, principal investigator (University of Calgary, Alberta, CA).
- Mr. Loic Tetrel, data scientist (CRIUGM, Quebec, CA).

CHAPTER

FOUR

MRI

4.1 Image acquisition

COMPASS-ND participants are scanned using the Canadian Dementia Imaging Protocol (CDIP). CDIP is organized around a central, tri-vendor (GE Healthcare, Philips Medical and Siemens Medical Systems MRI) harmonized core protocol of acquisitions. It is compressed to fit a 45-minutes window, which consists of six sequences:

- 3D T1-weighted
- T2/PD-weighted
- FLAIR
- T2*
- Diffusion imaging
- BOLD connectivity (resting state)

Prrovided below are the CDIP protocols for the:

- GE
- Philips Achieva and Philips Ingenia
- Siemens TRIO and Siemens PRISMA

3D T1-weighted scan

3D isotropic T1-weighted (T1w) imaging were obtained for assessing fine anatomical detail with high resolution (voxel size=1.0×1.0×1.0mm3) and acceleration factor of 2 (GE: FSPGR; Philips: T1-TFE; Siemens: MP-RAGE).

Table 1: MRI sites parameters

Site	Field Strength (T)	Voxel size (mm3)	Matrix size	Flip Angle	TE (s)	TR (s)
THE_OTTAWA_HOSPITAL_CIVIC	3	3	256x256	165	0.091	3
Civic_Hospital	3	3	256x256	165	0.091	3
UBC	3	3	256x256	90	0.1	3
UBC_MRI_Research_Centre	3	3	256x256	90	0.1	3
Hospital_Douglas	3	3	256x256	165	0.093	3
IRM_Quebec_-_Mailloux_-_3T	3	3	256x256	90	0.1	3
IRM_Quebec_-_Synase_-_3T	3	3	256x256	90	0.1	3
ST_JOSEPH_HAMILTON	3	3	256x256	125	0.085696	3
FOOTHILLS_Hospital	3	3	256x256	125	0.089792	3
CHUS_FLEURIMONT_Philips_3t	3	3	256x256	90	0.1	3
IUGM	3	3	256x256	165	0.093	3
Sunnybrook_Research_Institute	3	3	256x256	165	0.093	3
Robarts_Research_Institute	3	3	256x256	165	0.093	3
Robarts	3	3	256x256	165	0.093	3
Robarts-CFMM	3	3	256x256	165	0.093	3
3T_ROYAL_UNIVERSITY_HOSP	3	3	256x256	165	0.093	3
Toronto_Western	3	3	256x256	90	0.084544	3
Peter_S._Allen_MR_Research_Centre	3	3	256x256	165	0.093	3
WCMI_UPTOWN	3	3	256x256	142	0.086184	3.35

Resting-state Functional MRI (rsfMRI)

Functional T2*-weighted images are obtained using a blood-oxygen-level-dependent (BOLD) sensitive single-shot echo-planar (EPI) sequence on the GE Healthcare, Philips Medical or Siemens Medical Systems MRI scanners. During the rsfMRI acquisitions, no specific cognitive tasks are performed, and participants are instructed to keep their eyes open. No camera or physiological recordings are captured, as these equipments are not available at every site.

Table 2: f-MRI sites parameters

Site	Field Strength (T)	Voxel size (mm3)	Matrix size	Flip Angle	TE (s)	TR (s)	Volumes	Scan slices order	Scan time (min)
THE_OTTAWA_HOSPITAL_CIVIC	3	3.5	64x64	70	0.03	2.11	250	sequential decreasing	8.79
Civic_Hospital	3	3.5	64x64	70	0.03	2.11	250	sequential decreasing	8.79
UBC	3	3.5	64x64	70	0.03	2.11	250	unknown	8.79
UBC_MRI_Research_Centre	3	3.5	64x64	70	0.03	2.11	250	unknown	8.79
Hospital_Douglas	3	3.5	64x64	70	0.03	2.13	250	sequential decreasing	8.88
IRM_Quebec_-_Mailloux_-_3T	3	3.5	64x64	70	0.03	2.11	250	unknown	8.79
IRM_Quebec_-_Synase_-_3T	3	3.5	64x64	70	0.03	2.11	250	unknown	8.79
ST_JOSEPH_HAMILTON	3	3.5	64x64	70	0.03	2.4	200	unknown	8.00
FOOTHILLS_Hospital	3	3.5	64x64	70	0.03	2.5	200	unknown	8.33
CHUS_FLEURIMONT_Philips_3T	3	3.5	64x64	70	0.03	2.11	250	unknown	8.79
IUGM	3	3.5	64x64	70	0.03	2.13	250	sequential increasing	8.88
Sunnybrook_Research_Institute	3	3.5	64x64	70	0.03	2.13	250	sequential increasing	8.88
Robarts_Research_Institute	3	3.5	64x64	70	0.03	2.13	250	sequential increasing	8.88
Robarts	3	3.5	64x64	70	0.03	2.13	250	sequential increasing	8.88
Robarts-CFMM	3	3.5	64x64	70	0.03	2.13	250	sequential increasing	8.88
3T_ROYAL_UNIVERSITY_HOSP	3	3.5	64x64	70	0.03	2.67	250	sequential decreasing	11.12
Toronto_Western	3	3.5	64x64	70	0.03	2.4	250	unknown	10.00
Peter_S._Allen_MR_Research_Centre	3	3.5	64x64	70	0.03	2.24	250	sequential increasing	9.33
WCMI_UPTOWN	3	3.5	64x64	70	0.03	2.5	250	unknown	10.42

Diffusion weighted MRI (DWI)

Diffusion weighted images are obtained by measuring the random Brownian motion of water molecules within a voxel of tissue.

Table 3: DWI sites parameters

Site	Field Strength (T)	Voxel size (mm3)	Matrix size	TE (s)	TR (s)	b-values	Number of directions	Number of b0s	revb0
THE_OTTAWA_HOSPITAL_CIVIC	3	8	128x128	0.096	9.40	1000	30	1	none
Civic_Hospital	3	8	128x128	0.100	9.94	1000	32	1	none
UBC	3	8	128x128	0.100	9.93	1000	32	1	none
UBC_MRI_Research_Centre	3	8	128x128	0.096	9.40	1000	30	1	none
Hospital_Douglas	3	8	128x128	0.097	9.53	1000	32	1	none
IRM_Quebec_-_Mailloux_-_3T	3	8	128x128	0.097	9.53	1000	32	1	none
IRM_Quebec_-_Synase_-_3T	3	8	128x128	0.085	9.00	1000	30	3	none
ST_JOSEPH_HAMILTON	3	8	128x128	0.087	9.00	1000	30	3	none
FOOTHILLS_Hospital	3	8	128x128	0.109	10.44	1000	32	1	none
CHUS_FLEURIMONT_Philips_3t	3	8	128x128	0.064	6.90	1000	30	3	none
IUGM	3	8	128x128	0.064	6.90	1000	30	3	none
Sunnybrook_Research_Institute	3	8	128x128	0.064	6.90	1000	30	3	none
Robarts_Research_Institute	3	8	128x128	0.064	6.90	1000	30	3	none
Robarts	3	8	128x128	0.064	6.90	1000	30	3	none
Robarts-CFMM	3	8	128x128	0.101	13.00	1000	30	1	none
3T_ROYAL_UNIVERSITY_HOSP	3	8	128x128	0.106	11.70	1000	30	3	none
Toronto_Western	3	8	128x128	0.064	6.90	1000	30	3	none
Peter_S._Allen_MR_Research_Centre	3	8	128x128	0.083	12.50	1000	30	3	none
WCMI_UPTOWN	3	1	256x256	0.064	6.90	1000	30	1	none

CHAPTER

FIVE

RESTING-STATE FUNCTIONAL MRI (RSFMRI)

Synaptic dysfunction has long been hypothesized to be an early event in AD degeneration, and is likely to be reflected in fMRI connectivity. To derive a functional connectivity map, one needs to specify an anatomical location, or use some data driven technique such as a bootstrap analysis of stable clusters (BASC) (Bellec et al. 2010) to generate a group template of resting-state networks, here the DMN (panel a). Average time series within the target region/network are derived from a series of individual datasets (panel b), and correlated with the time series of all voxels across the brain, resulting into individual fc-maps (panel c). Promising results were first reported in the literature on cross-sectional comparisons of fc-maps between patients with AD dementia and cognitively normal (CN) elderly subjects (e.g. REFS), as well a comparisons of patients with MCI of the amnestic type and CN (e.g.). Although most published studies feature low sample size, two recent meta-analysis from my group, one combining imaging data of N=255 in CN and MCI participants across four studies (Tam et al. 2015), and another one combining published coordinates from 34 published studies, including N=1363 individuals, point to a consistent dysconnectivity in regions of the default-mode network, as well as alterations in limbic and fronto-parietal networks. In addition to these clinical comparisons, several studies have reported differences in resting-state connectivity between amyloid beta positive vs negative CN elderly subjects, e.g. (Sheline et al. 2010), as well as differences between CN participants with and without a family history of AD. Overall, despite still being in its infancy, there is solid evidence at this stage in the literature that rs-fMRI is an early, sensitive marker of the progression of AD (Vemuri, Jones, and Jack 2012).

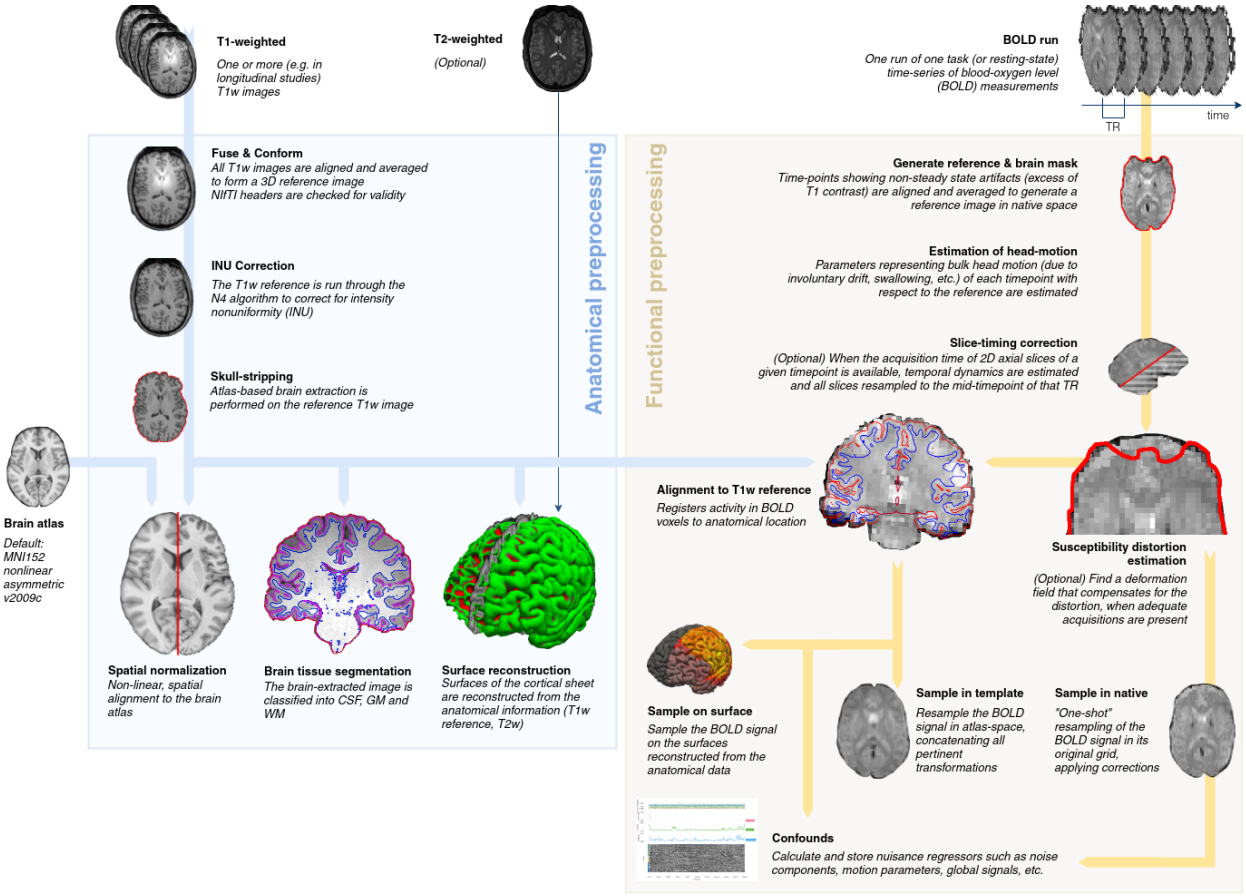

5.1 fMRIprep Pipeline

The fMRIprep pipeline, developed by the Poldrack lab at Stanford University, performs basic processing steps (coregistration, normalization, unwarping, noise component extraction, segmentation, skullstripping etc.) providing outputs that can be easily submitted to a variety of group level analyses, including task-based or resting-state fMRI, graph theory measures, surface or volume-based statistics, etc. The fMRIPrep pipeline uses a combination of tools from well-known software packages, including FSL, ANTs, FreeSurfer and AFNI. This pipeline was designed to provide the best software implementation for each state of preprocessing.

The CCNA dataset is processed using fMRIprep version 20.2.1 LTS, which is based on Nipype 1.5.1. Many internal operations of fMRIPrep use Nilearn 0.6.2, mostly within the functional processing workflow. For more details of the pipeline, see [the section corresponding to workflows in fMRIPrep's documentation](https://fmriprep.readthedocs.io/en/latest/workflows.html "FMRIPrep's documentation"). Processing scripts will be made available on github. A full description The log files for execution will be included with the derivatives and can be accessed through the PSOM interface.

5.1.1 Structural processing

The T1-weighted (T1w) images were corrected for intensity non-uniformity (INU) with *N4BiasFieldCorrection*, distributed with ANTs 2.3.3, and used as T1w-reference throughout the workflow. The T1w-reference was then skullstripped with a Nipype implementation of the *antsBrainExtraction.sh* workflow (from ANTs), using OASIS30ANTs as target template. Brain tissue segmentation of cerebrospinal fluid (CSF), white-matter (WM) and gray-matter (GM) were performed on the brain-extracted T1w using *fast* (FSL 5.0.9). Brain surfaces were reconstructed using *recon-all*

(FreeSurfer 6.0.1), and the brain mask estimated previously was refined with a custom variation of the method to reconcile ANTs-derived and FreeSurfer-derived segmentations of the cortical gray-matter of Mindboggle. Volume-based spatial normalization to two standard spaces (MNI152NLin2009cAsym, MNI152NLin6Asym) was performed through nonlinear registration with *antsRegistration* (ANTs 2.3.3), using brain-extracted versions of both T1w reference and the T1w template. The following templates were selected for spatial normalization: ICBM 152 Nonlinear Asymmetrical template version 2009c, and FSL's MNI ICBM 152 non-linear 6th Generation Asymmetric Average Brain Stereotaxic Registration Model.

Note: For more information on the Freesurfer steps and processing please see the section on sMRI.

5.1.2 Functional processing

Preprocessing

For each of the 1 BOLD runs found per subject (across all tasks and sessions), the following preprocessing was performed. First, a reference volume and its skull-stripped version were generated using a custom methodology of fMRIPrep. Susceptibility distortion correction (SDC) was omitted. The BOLD reference was then co-registered to the T1w reference using *bbregister* (FreeSurfer) which implements boundary-based registration. Co-registration was configured with six degrees of freedom. Head-motion parameters with respect to the BOLD reference (transformation matrices, and six corresponding rotation and translation parameters) are estimated before any spatiotemporal filtering using *mcflirt* (FSL 5.0.9). BOLD runs were slice-time corrected using *3dTshift* from AFNI 20160207. The BOLD time-series (including slice-timing correction when applied) were resampled onto their original, native space by applying the transforms to correct for head-motion. These resampled BOLD time-series will be referred to as preprocessed BOLD in original space, or just preprocessed BOLD. The BOLD time-series were resampled into standard space, generating a preprocessed BOLD run in MNI152NLin2009cAsym space. A reference volume and its skull-stripped version were generated using a custom methodology of fMRIPrep.

Automatic removal of motion artifacts using independent component analysis

Automatic removal of motion artifacts using independent component analysis (ICA-AROMA) was performed on the preprocessed BOLD on MNI space time-series after removal of non-steady state volumes and spatial smoothing with an isotropic, Gaussian kernel of 6mm FWHM (full-width half-maximum). Corresponding "non-aggresively" denoised runs were produced after such smoothing. Additionally, the "aggressive" noise-regressors were collected and placed in the corresponding confounds file. Several confounding time-series were calculated based on the preprocessed BOLD: framewise displacement (FD), DVARS and three region-wise global signals. FD was computed using two formulations following Power (absolute sum of relative motions, power_fd_dvars) and Jenkinson (relative root mean square displacement between affines, mcflirt). FD and DVARS are calculated for each functional run, both using their implementations in Nipype (following the definitions by 9power_fd_dvars). The three global signals are extracted within the CSF, the WM, and the whole-brain masks.

Additionally, a set of physiological regressors were extracted to allow for component-based noise correction (CompCor). Principal components are estimated after high-pass filtering the preprocessed BOLD time-series (using a discrete cosine filter with 128s cut-off) for the two CompCor variants: temporal (tCompCor) and anatomical (aCompCor). tCompCor components are then calculated from the top 2% variable voxels within the brain mask. For aCompCor, three probabilistic masks (CSF, WM and combined CSF+WM) are generated in anatomical space. The implementation differs from that of Behzadi et al. in that instead of eroding the masks by 2 pixels on BOLD space, the aCompCor masks are subtracted a mask of pixels that likely contain a volume fraction of GM. This mask is obtained by dilating a GM mask extracted from the FreeSurfer's aseg segmentation, and it ensures components are not extracted from voxels containing a minimal fraction of GM.

Finally, these masks are resampled into BOLD space and binarized by thresholding at 0.99 (as in the original implementation). Components are also calculated separately within the WM and CSF masks. For each CompCor de-

composition, the k components with the largest singular values are retained, such that the retained components' time series are sufficient to explain 50 percent of variance across the nuisance mask (CSF, WM, combined, or temporal). The remaining components are dropped from consideration. The head-motion estimates calculated in the correction step were also placed within the corresponding confounds file. The confound time series derived from head motion estimates and global signals were expanded with the inclusion of temporal derivatives and quadratic terms for each (confounds_satterthwaite_2013). Frames that exceeded a threshold of 0.5 mm FD or 1.5 standardised DVARS were annotated as motion outliers.

All resamplings can be performed with a single interpolation step by composing all the pertinent transformations (i.e. head-motion transform matrices, susceptibility distortion correction when available, and co-registrations to anatomical and output spaces). Gridded (volumetric) resamplings were performed using *antsApplyTransforms* (ANTs), configured with Lanczos interpolation to minimize the smoothing effects of other kernels. Non-gridded (surface) resamplings were performed using *mri_vol2surf* (FreeSurfer).

Copyright Waiver

The above processing boilerplate text was automatically generated by fMRIPrep with the express intention that users may copy and paste the text into their manuscripts unchanged. It is released under the [CC0](https://creativecommons.org/publicdomain/zero/1.0/) license.

5.1.3 Quality control

Outputs of the fMRIprep pipeline will be subjected to a careful visual inspection and the results quality calls, along with head motion statistics, will be made available on the fMRIprep description. Estimates of the maximum motion (translation and rotation) between consecutive functional volumes for each rs-fMRI dataset will be inspected to categorize the datasets as containing minimal (<1mm or degree), moderate (2 to 3 mm or degrees) or severe motion (>3 mm or degrees). The individual results of the fMRIprep pipeline will be visually inspected for quality of the registration between rs-fMRI and s-MRI data, registration of s-MRI data to template space, and for common artefacts such as ghosting and signal loss. In the case of identification of substandard registration outcomes, a parameter controlling the non-uniformity correction of the s-MRI will be adjusted and the analysis repeated until the coregistration results is satisfactory.

Quality control outputs will include:

- motion statistics distributed in comma-seperated values format (.csv) for each site
- average structural scans after linear and non-linear transformations in compressed nifti format (.nii.gz).
- average functional scans after linear and non-linear transformations in compressed nifti format
- average of all anatomical brain masks for each site of the training and test samples in compressed nifti format (.nii.gz)
- average of all functional brain masks for each site of the training and test samples are included as compressed nifti format (.nii.gz)

> **Note:** Packages for quality control: registration in particular

http://www.nitrc.org/plugins/mwiki/index.php/neurobureau:fMRIprepPipeline http://www.nitrc.org/frs/?group_id=411 https://github.com/SIMEXP/fmriprep http://psom.simexp-lab.org/how_to_use_psom.html

CHAPTER

SIX

DIFFUSION MRI (DMRI)

TractoFlow pipeline is developed by the Sherbrooke Connectivity Imaging Lab (SCIL) in order to process diffusion MRI dataset from the raw data to the tractography. The pipeline is based on Nextflow and Singularity. The goal with this pipeline is to be fast and reproducible.

Use TractoFlow in published works should be accompanied by the following citation:

> Theaud, G., Houde, J.-C., Boré, A., Rheault, F., Morency, F., Descoteaux, M.,TractoFlow: A robust, efficient and reproducible diffusion MRI pipeline leveraging Nextflow & Singularity, NeuroImage, https://doi.org/10.1016/j.neuroimage.2020.116889.

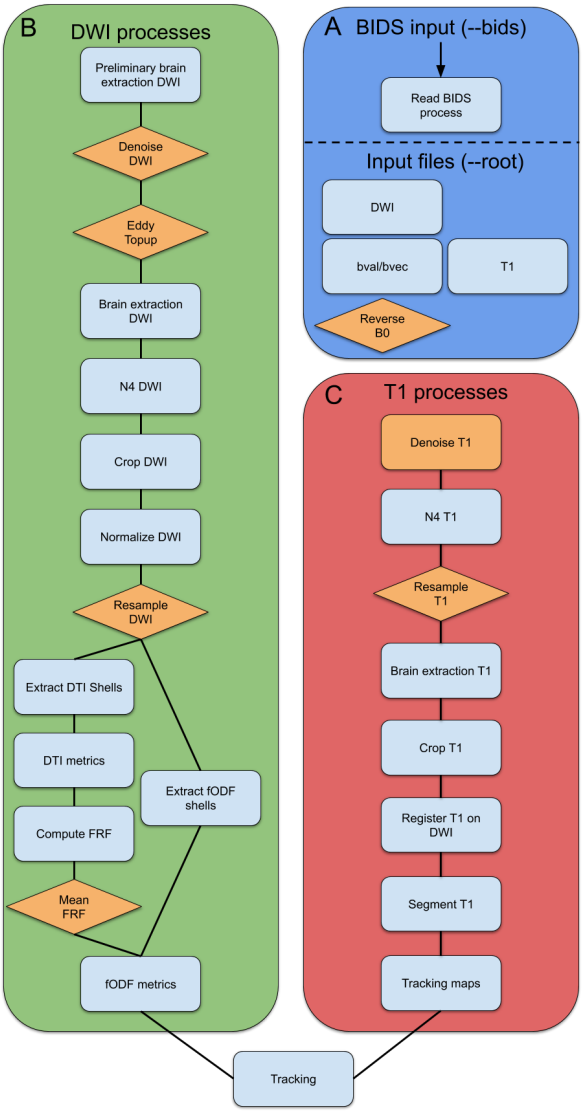

6.1 TractoFlow pipeline

TractoFlow pipeline consist of 23 different steps : 14 steps for the diffusion weighted image (DWI) processing and 8 steps for the T1 weighted image processing.

6.1.1 Input

- Diffusion weighted image (DWI)
- b-values
- b-vectors
- T1 weighted image
- Reverse phase encoding B0 (Optional)

6.1.2 DWI processes

- Brain extraction (FSL)
- Denoising (Mrtrix3)
- Topup (FSL)
- Eddy (FSL)
- N4 bias correction (ANTs)
- Resample (Dipy)
- DTI metrics (Dipy)
- fODF metrics (Dipy)

6.1.3 T1 processes

- Brain extraction (ANTs)
- Denoising (Dipy)
- N4 bias correction (ANTs)
- Resample (Dipy)
- Registration (ANTs)
- Tissue segmentation (FSL)

6.1.4 Tractography

The particle filter tractography is performed. Two types of seeding are available: WM-GM interface or WM mask.

CHAPTER

SEVEN

STRUCTURAL MRI (SMRI)

7.1 Freesurfer Pipeline

Cortical reconstruction and volumetric segmentation was performed with the Freesurfer image analysis suite, which is documented and freely available for download online (http://surfer.nmr.mgh.harvard.edu/). The technical details of these procedures are described in prior publications (Dale et al., 1999; Dale and Sereno, 1993; Fischl and Dale, 2000; Fischl et al., 2001; Fischl et al., 2002; Fischl et al., 2004a; Fischl et al., 1999a; Fischl et al., 1999b; Fischl et al., 2004b; Han et al., 2006; Jovicich et al., 2006; Segonne et al., 2004, Reuter et al. 2010, Reuter et al. 2012). Briefly, this processing includes motion correction and averaging (Reuter et al. 2010) of multiple volumetric T1 weighted images (when more than one is available), removal of non-brain tissue using a hybrid watershed/surface deformation procedure (Segonne et al., 2004), automated Talairach transformation, segmentation of the subcortical white matter and deep gray matter volumetric structures (including hippocampus, amygdala, caudate, putamen, ventricles) (Fischl et al., 2002; Fischl et al., 2004a) intensity normalization (Sled et al., 1998), tessellation of the gray matter white matter boundary, automated topology correction (Fischl et al., 2001; Segonne et al., 2007), and surface deformation following intensity gradients to optimally place the gray/white and gray/cerebrospinal fluid borders at the location where the greatest shift in intensity defines the transition to the other tissue class (Dale et al., 1999; Dale and Sereno, 1993; Fischl and Dale, 2000). Once the cortical models are complete, a number of deformable procedures can be performed for further data processing and analysis including surface inflation (Fischl et al., 1999a), registration to a spherical atlas which is based on individual cortical folding patterns to match cortical geometry across subjects (Fischl et al., 1999b), parcellation of the cerebral cortex into units with respect to gyral and sulcal structure (Desikan et al., 2006; Fischl et al., 2004b), and creation of a variety of surface based data including maps of curvature and sulcal depth. This method uses both intensity and continuity information from the entire three dimensional MR volume in segmentation and deformation procedures to produce representations of cortical thickness, calculated as the closest distance from the gray/white boundary to the gray/CSF boundary at each vertex on the tessellated surface (Fischl and Dale, 2000). The maps are created using spatial intensity gradients across tissue classes and are therefore not simply reliant on absolute signal intensity. The maps produced are not restricted to the voxel resolution of the original data thus are capable of detecting submillimeter differences between groups. Procedures for the measurement of cortical thickness have been validated against histological analysis (Rosas et al., 2002) and manual measurements (Kuperberg et al., 2003; Salat et al., 2004). Freesurfer morphometric procedures have been demonstrated to show good test-retest reliability across scanner manufacturers and across field strengths (Han et al., 2006; Reuter et al., 2012).

7.1.1 Aseg Atlas Information

The aseg atlas is built from 40 subjects acquired using the same mp-rage sequence (by people at Wash U ages ago in collaboration with Randy Buckner). The subjects that make up the atlas are distributed in 4 groups of 10 subjects each: (1) young, (2) middle aged, (3) healthy older adults, (4) older adults with AD.

Quality Control

Quality control images are generated using post-processing showing selected slices of input images overlayed with candidate segmentations. Quality control must be performed manually by the user to confirm successful segmentation.

Freesurfer derivatives

Freesurfer output files may be found in the freesurfer directory under the individual subject folders.

```
/mri/orig
 001.mgz
 002.mgz
 T1raw.mgz
/mri
 rawavg.mgz
 orig.mgz
 orig_nu.mgz
 nu.mgz
 T1.mgz
 brainmask.mgz
 norm.mgz
 aseg.auto.mgz
 aseg.presurf.mgz
 brain.mgz
 brain.finalsurfs.mgz
 wm.mgz
 filled.mgz
 aparc+aseg.mgz
 aparc.a2009s+aseg.mgz
 aparc.DKTatlas+aseg.mgz
 aseg.mgz
 wmparc.mgz
/mri/transforms
 talairach.xfm
 talairach_with_skull.lta
 talairach.lta
 talairach.m3z
/surf
 ?h.orig.nofix
 ?h.smoothwm.nofix
 ?h.inflated.nofix
 ?h.qsphere.nofix
 ?h.orig
 ?h.inflated
/labels
 ?h.aparc.annot
 ?h.cortex.label
 ?h.*_exvivo.label
/stats
 ?h.aparc.stats
 aseg.stats
 wmparc.stats
 ?h.BA_exvivo.stats
/scripts
 recon-all.log
 build-stamp.txt
 lastcall.build-stamp.txt
```

(continues on next page)

(continued from previous page)

```
recon-all.env
recon-all.cmd
recon-all.done
recon-all-status.log
```

The above processing boilerplate text was taken from the Freesurfer Methods Citation site at: https://surfer.nmr.mgh.harvard.edu/fswiki/FreeSurferMethodsCitation

Freesurfer references

Dale, A.M., Fischl, B., Sereno, M.I., 1999. Cortical surface-based analysis. I. Segmentation and surface reconstruction. Neuroimage 9, 179-194.

Dale, A.M., Sereno, M.I., 1993. Improved localization of cortical activity by combining EEG and MEG with MRI cortical surface reconstruction: a linear approach. J Cogn Neurosci 5, 162-176.

Desikan, R.S., Segonne, F., Fischl, B., Quinn, B.T., Dickerson, B.C., Blacker, D., Buckner, R.L., Dale, A.M., Maguire, R.P., Hyman, B.T., Albert, M.S., Killiany, R.J., 2006. An automated labeling system for subdividing the human cerebral cortex on MRI scans into gyral based regions of interest. Neuroimage 31, 968-980.

Fischl, B., Dale, A.M., 2000. Measuring the thickness of the human cerebral cortex from magnetic resonance images. Proc Natl Acad Sci U S A 97, 11050-11055.

Fischl, B., Liu, A., Dale, A.M., 2001. Automated manifold surgery: constructing geometrically accurate and topologically correct models of the human cerebral cortex. IEEE Trans Med Imaging 20, 70-80.

Fischl, B., Salat, D.H., Busa, E., Albert, M., Dieterich, M., Haselgrove, C., van der Kouwe, A., Killiany, R., Kennedy, D., Klaveness, S., Montillo, A., Makris, N., Rosen, B., Dale, A.M., 2002. Whole brain segmentation: automated labeling of neuroanatomical structures in the human brain. Neuron 33, 341-355.

Fischl, B., Salat, D.H., van der Kouwe, A.J., Makris, N., Segonne, F., Quinn, B.T., Dale, A.M., 2004a. Sequence-independent segmentation of magnetic resonance images. Neuroimage 23 Suppl 1, S69-84.

Fischl, B., Sereno, M.I., Dale, A.M., 1999a. Cortical surface-based analysis. II: Inflation, flattening, and a surface-based coordinate system. Neuroimage 9, 195-207.

Fischl, B., Sereno, M.I., Tootell, R.B., Dale, A.M., 1999b. High-resolution intersubject averaging and a coordinate system for the cortical surface. Hum Brain Mapp 8, 272-284.

Fischl, B., van der Kouwe, A., Destrieux, C., Halgren, E., Segonne, F., Salat, D.H., Busa, E., Seidman, L.J., Goldstein, J., Kennedy, D., Caviness, V., Makris, N., Rosen, B., Dale, A.M., 2004b. Automatically parcellating the human cerebral cortex. Cereb Cortex 14, 11-22.

Han, X., Jovicich, J., Salat, D., van der Kouwe, A., Quinn, B., Czanner, S., Busa, E., Pacheco, J., Albert, M., Killiany, R., Maguire, P., Rosas, D., Makris, N., Dale, A., Dickerson, B., Fischl, B., 2006. Reliability of MRI-derived measurements of human cerebral cortical thickness: the effects of field strength, scanner upgrade and manufacturer. Neuroimage 32, 180-194.

Jovicich, J., Czanner, S., Greve, D., Haley, E., van der Kouwe, A., Gollub, R., Kennedy, D., Schmitt, F., Brown, G., Macfall, J., Fischl, B., Dale, A., 2006. Reliability in multi-site structural MRI studies: effects of gradient non-linearity correction on phantom and human data. Neuroimage 30, 436-443.

Kuperberg, G.R., Broome, M.R., McGuire, P.K., David, A.S., Eddy, M., Ozawa, F., Goff, D., West, W.C., Williams, S.C., van der Kouwe, A.J., Salat, D.H., Dale, A.M., Fischl, B., 2003. Regionally localized thinning of the cerebral cortex in schizophrenia. Arch Gen Psychiatry 60, 878-888.

Reuter, M., Schmansky, N.J., Rosas, H.D., Fischl, B. 2012. Within-Subject Template Estimation for Unbiased Longitudinal Image Analysis. Neuroimage 61 (4), 1402-1418. http://reuter.mit.edu/papers/reuter-long12.pdf

Reuter, M., Fischl, B., 2011. Avoiding asymmetry-induced bias in longitudinal image processing. Neuroimage 57 (1), 19-21. http://reuter.mit.edu/papers/reuter-bias11.pdf

Reuter, M., Rosas, H.D., Fischl, B., 2010. Highly Accurate Inverse Consistent Registration: A Robust Approach. Neuroimage 53 (4), 1181–1196. http://reuter.mit.edu/papers/reuter-robreg10.pdf

Rosas, H.D., Liu, A.K., Hersch, S., Glessner, M., Ferrante, R.J., Salat, D.H., van der Kouwe, A., Jenkins, B.G., Dale, A.M., Fischl, B., 2002. Regional and progressive thinning of the cortical ribbon in Huntington's disease. Neurology 58, 695-701.

Salat, D.H., Buckner, R.L., Snyder, A.Z., Greve, D.N., Desikan, R.S., Busa, E., Morris, J.C., Dale, A.M., Fischl, B., 2004. Thinning of the cerebral cortex in aging. Cereb Cortex 14, 721-730.

Segonne, F., Dale, A.M., Busa, E., Glessner, M., Salat, D., Hahn, H.K., Fischl, B., 2004. A hybrid approach to the skull stripping problem in MRI. Neuroimage 22, 1060-1075.

Segonne, F., Pacheco, J., Fischl, B., 2007. Geometrically accurate topology-correction of cortical surfaces using nonseparating loops. IEEE Trans Med Imaging 26, 518-529.

Sled, J.G., Zijdenbos, A.P., Evans, A.C., 1998. A nonparametric method for automatic correction of intensity nonuniformity in MRI data. IEEE Trans Med Imaging 17, 87-97.

CHAPTER

EIGHT

REFERENCES

1http://www.nitrc.org/plugins/mwiki/index.php/neurobureau:NIAKPipeline 2http://en.wikibooks.org/wiki/MINC 3http://www.nitrc.org/frs/?group_id=411 4https://github.com/SIMEXP/niak 5http://psom.simexp-lab.org/how_to_use_psom.html

Aganj, Iman, Christophe Lenglet, Guillermo Sapiro, Essa Yacoub, Kamil Ugurbil, and Noam Harel. 2010. "Reconstruction of the Orientation Distribution Function in Single- and Multiple-Shell Q-Ball Imaging within Constant Solid Angle." Magnetic Resonance in Medicine: Official Journal of the Society of Magnetic Resonance in Medicine / Society of Magnetic Resonance in Medicine 64 (2): 554–66.

Andersson, Jesper L. R., and Stamatios N. Sotiropoulos. 2016. "An Integrated Approach to Correction for off-Resonance Effects and Subject Movement in Diffusion MR Imaging." NeuroImage 125 (January): 1063–78.

Bellec, Pierre, Sébastien Lavoie-Courchesne, Phil Dickinson, Jason Lerch, Alex Zijdenbos, and Alan C. Evans. 2012. "The Pipeline System for Octave and Matlab (PSOM): A Lightweight Scripting Framework and Execution Engine for Scientific Workflows." Frontiers in Neuroinformatics 6 (March). Frontiers. doi:10.3389/fninf.2012.00007.

Bellec, Pierre, Vincent Perlbarg, Saâd Jbabdi, Mélanie Pélégrini-Issac, Jean-Luc Anton, Julien Doyon, and Habib Benali. 2006. "Identification of Large-Scale Networks in the Brain Using fMRI." NeuroImage 29 (4): 1231–43.

Calamante, Fernando, Robert E. Smith, Jacques-Donald Tournier, David Raffelt, and Alan Connelly. 2015. "Quantification of Voxel-Wise Total Fibre Density: Investigating the Problems Associated with Track-Count Mapping." NeuroImage 117 (August): 284–93.

Calamante, Fernando, Jacques-Donald Tournier, Graeme D. Jackson, and Alan Connelly. 2010. "Track-Density Imaging (TDI): Super-Resolution White Matter Imaging Using Whole-Brain Track-Density Mapping." NeuroImage 53 (4): 1233–43.

Chen, Z., R. Camicioli, H. Zhang, C. L. Yasuda, and C. Beaulieu. 2016. "Longitudinal Diffusion Changes Along White Matter Tract Surfaces in Alzheimer's Disease." In International Conference on Promoting Healthy Brain Aging and Preventing Dementia.

Chen, Zhang, Hui Zhang, Paul A. Yushkevich, Min Liu, and Christian Beaulieu. 2016. "Maturation Along White Matter Tracts in Human Brain Using a Diffusion Tensor Surface Model Tract-Specific Analysis." Frontiers in Neuroanatomy 10 (February): 9.

Chen, Z., H. Zhang, R. Camicioli, and C. Beaulieu. 2015. "Diffusion Changes Along White Matter Tract Surfaces in Alzheimer's Disease - an ADNI Cohort Study." In .

Colby, John B., Lindsay Soderberg, Catherine Lebel, Ivo D. Dinov, Paul M. Thompson, and Elizabeth R. Sowell. 2012. "Along-Tract Statistics Allow for Enhanced Tractography Analysis." NeuroImage 59 (4): 3227–42.

Collins, D. L., P. Neelin, T. M. Peters, and A. C. Evans. 1994. "Automatic 3D Intersubject Registration of MR Volumetric Data in Standardized Talairach Space." Journal of Computer Assisted Tomography 18 (2): 192–205.

Corouge, Isabelle, P. Thomas Fletcher, Sarang Joshi, Sylvain Gouttard, and Guido Gerig. 2006. "Fiber Tract-Oriented Statistics for Quantitative Diffusion Tensor MRI Analysis." Medical Image Analysis 10 (5): 786–98.

Dell'Acqua, Flavio, Andrew Simmons, Steven C. R. Williams, and Marco Catani. 2013. "Can Spherical Deconvolution Provide More Information than Fiber Orientations? Hindrance Modulated Orientational Anisotropy, a True-Tract Specific Index to Characterize White Matter Diffusion." Human Brain Mapping 34 (10): 2464–83.

Descoteaux, Maxime, Elaine Angelino, Shaun Fitzgibbons, and Rachid Deriche. 2007. "Regularized, Fast, and Robust Analytical Q-Ball Imaging." Magnetic Resonance in Medicine: Official Journal of the Society of Magnetic Resonance in Medicine / Society of Magnetic Resonance in Medicine 58 (3): 497–510.

Descoteaux, Maxime, Rachid Deriche, Thomas R. Knösche, and Alfred Anwander. 2009. "Deterministic and Probabilistic Tractography Based on Complex Fibre Orientation Distributions." IEEE Transactions on Medical Imaging 28 (2): 269–86.

Descoteaux, Maxime, and John G. Webster. 1999. "High Angular Resolution Diffusion Imaging (HARDI)." In Wiley Encyclopedia of Electrical and Electronics Engineering. John Wiley & Sons, Inc.

Descoteaux, Maxime, Nicolas Wiest-Daesslé, Sylvain Prima, Christian Barillot, and Rachid Deriche. 2008. "Impact of Rician Adapted Non-Local Means Filtering on HARDI." Medical Image Computing and Computer-Assisted Intervention: MICCAI ... International Conference on Medical Image Computing and Computer-Assisted Intervention 11 (Pt 2): 122–30.

Descoteaux, M., and C. Poupon. 2014. "3.06 - Diffusion-Weighted MRI A2 - Brahme, Anders." In Comprehensive Biomedical Physics, 81–97. Oxford: Elsevier.

Fonov, Vladimir, Alan C. Evans, Kelly Botteron, C. Robert Almli, Robert C. McKinstry, D. Louis Collins, and Brain Development Cooperative Group. 2011. "Unbiased Average Age-Appropriate Atlases for Pediatric Studies." NeuroImage 54 (1): 313–27.

Garyfallidis, Eleftherios, Matthew Brett, Bagrat Amirbekian, Ariel Rokem, Stefan van der Walt, Maxime Descoteaux, Ian Nimmo-Smith, and Dipy Contributors. 2014. "Dipy, a Library for the Analysis of Diffusion MRI Data." Frontiers in Neuroinformatics 8 (February): 8.

Girard, Gabriel, Kevin Whittingstall, Rachid Deriche, and Maxime Descoteaux. 2014. "Towards Quantitative Connectivity Analysis: Reducing Tractography Biases." NeuroImage 98 (September): 266–78.

Goodlett, Casey B., P. Thomas Fletcher, John H. Gilmore, and Guido Gerig. 2009. "Group Analysis of DTI Fiber Tract Statistics with Application to Neurodevelopment." NeuroImage 45 (1 Suppl): S133–42.

Lebel, Catherine, Carmen Rasmussen, Katy Wyper, Lindsay Walker, Gail Andrew, Jerome Yager, and Christian Beaulieu. 2008. "Brain Diffusion Abnormalities in Children with Fetal Alcohol Spectrum Disorder." Alcoholism, Clinical and Experimental Research 32 (10): 1732–40.

Lebel, C., M. Gee, R. Camicioli, M. Wieler, W. Martin, and C. Beaulieu. 2012. "Diffusion Tensor Imaging of White Matter Tract Evolution over the Lifespan." NeuroImage 60 (1): 340–52.

Nir, Talia M., Julio E. Villalon-Reina, Gautam Prasad, Neda Jahanshad, Shantanu H. Joshi, Arthur W. Toga, Matt A. Bernstein, et al. 2015. "Diffusion Weighted Imaging-Based Maximum Density Path Analysis and Classification of Alzheimer's Disease." Neurobiology of Aging 36 Suppl 1 (January): S132–40.

O'Donnell, Lauren J., Carl-Fredrik Westin, and Alexandra J. Golby. 2009. "Tract-Based Morphometry for White Matter Group Analysis." NeuroImage 45 (3): 832–44.

Oguz, Ipek, Mahshid Farzinfar, Joy Matsui, Francois Budin, Zhexing Liu, Guido Gerig, Hans J. Johnson, and Martin Styner. 2014. "DTIPrep: Quality Control of Diffusion-Weighted Images." Frontiers in Neuroinformatics 8 (January): 4.

Park, Jong Geun, and Chulhee Lee. 2009. "Skull Stripping Based on Region Growing for Magnetic Resonance Brain Images." NeuroImage 47 (4): 1394–1407.

Perlbarg, Vincent, Pierre Bellec, Jean-Luc Anton, Mélanie Pélégrini-Issac, Julien Doyon, and Habib Benali. 2007. "CORSICA: Correction of Structured Noise in fMRI by Automatic Identification of ICA Components." Magnetic Resonance Imaging 25 (1): 35–46.

Raffelt, David, J-Donald Tournier, Stephen Rose, Gerard R. Ridgway, Robert Henderson, Stuart Crozier, Olivier Salvado, and Alan Connelly. 2012. "Apparent Fibre Density: A Novel Measure for the Analysis of Diffusion-Weighted Magnetic Resonance Images." NeuroImage 59 (4): 3976–94.

Ray, Kimberly M., Huali Wang, Yong Chu, Ya-Fang Chen, Alberto Bert, Anton N. Hasso, and Min-Ying Su. 2006. "Mild Cognitive Impairment: Apparent Diffusion Coefficient in Regional Gray Matter and White Matter Structures." Radiology 241 (1): 197–205.

Rovaris, M., E. Judica, A. Gallo, B. Benedetti, M. P. Sormani, D. Caputo, A. Ghezzi, et al. 2006. "Grey Matter Damage Predicts the Evolution of Primary Progressive Multiple Sclerosis at 5 Years." Brain: A Journal of Neurology 129 (Pt 10): 2628–34.

Shaw, Philip, Jason Lerch, Deanna Greenstein, Wendy Sharp, Liv Clasen, Alan Evans, Jay Giedd, F. Xavier Castellanos, and Judith Rapoport. 2006. "Longitudinal Mapping of Cortical Thickness and Clinical Outcome in Children and Adolescents with Attention-Deficit/hyperactivity Disorder." Archives of General Psychiatry 63 (5): 540–49.

Sherif, Tarek, Pierre Rioux, Marc-Etienne Rousseau, Nicolas Kassis, Natacha Beck, Reza Adalat, Samir Das, Tristan Glatard, and Alan C. Evans. 2014. "CBRAIN: A Web-Based, Distributed Computing Platform for Collaborative Neuroimaging Research." Frontiers in Neuroinformatics 8 (April). Frontiers. doi:10.3389/fninf.2014.00054.

Sled, J. G., A. P. Zijdenbos, and A. C. Evans. 1998. "A Nonparametric Method for Automatic Correction of Intensity Nonuniformity in MRI Data." IEEE Transactions on Medical Imaging 17 (1): 87–97.

Tournier, J-Donald, Fernando Calamante, and Alan Connelly. 2007. "Robust Determination of the Fibre Orientation Distribution in Diffusion MRI: Non-Negativity Constrained Super-Resolved Spherical Deconvolution." NeuroImage 35 (4): 1459–72.

Tuch, David S. 2004. "Q-Ball Imaging." Magnetic Resonance in Medicine: Official Journal of the Society of Magnetic Resonance in Medicine / Society of Magnetic Resonance in Medicine 52 (6): 1358–72.

Tzourio-Mazoyer, N., B. Landeau, D. Papathanassiou, F. Crivello, O. Etard, N. Delcroix, B. Mazoyer, and M. Joliot. 2002. "Automated Anatomical Labeling of Activations in SPM Using a Macroscopic Anatomical Parcellation of the MNI MRI Single-Subject Brain." NeuroImage 15 (1): 273–89.

Yushkevich, Paul A., Hui Zhang, and James C. Gee. 2006. "Continuous Medial Representation for Anatomical Structures." IEEE Transactions on Medical Imaging 25 (12): 1547–64.

Yushkevich, Paul A., Hui Zhang, Tony J. Simon, and James C. Gee. 2008. "Structure-Specific Statistical Mapping of White Matter Tracts." NeuroImage 41 (2): 448–61.

CHAPTER

NINE

INDICES AND TABLES

- genindex
- modindex
- search